

# Braess paradox and quantum interference in simple quantum graphs

A. Drinko,<sup>1,\*</sup> F. M. Andrade,<sup>1,2,†</sup> and D. Bazeia<sup>3,‡</sup>

<sup>1</sup>*Programa de Pós-Graduação em Ciências/Física, Universidade Estadual de Ponta Grossa, 84030-900 Ponta Grossa, PR, Brazil*

<sup>2</sup>*Departamento de Matemática e Estatística, Universidade Estadual de Ponta Grossa, 84030-900 Ponta Grossa, PR, Brazil*

<sup>3</sup>*Departamento de Física, Universidade Federal da Paraíba 58051-900 João Pessoa, PB, Brazil*

(Dated: July 2, 2019)

This work deals with quantum graphs, focusing on the transmission properties they engender. We first select two simple graphs, in which the vertices are all of degree 3, and investigate their transmission coefficients. In particular, we identified regions in which the transmission is fully suppressed. We also considered the transmission coefficients of some series and parallel arrangements of the two basic graphs, with the vertices still preserving the degree 3 condition, and then identified specific series and parallel compositions that allow for windows of no transmission. Inside some of these windows, we found very narrow peaks of full transmission, which are consequences of constructive quantum interference. Possibilities of practical use, as the experimental construction of devices of current interest to control and manipulate quantum information are also discussed.

## I. INTRODUCTION

In the last twenty years, quantum graphs [1, 2] have been used to describe the behavior of quantum particles in idealized physical networks. The interest is due to the richness of the subject, which can be related to a variety of issues in physical and mathematical sciences. For instance, it has been simulated experimentally in microwave networks [3] and it is also possible to synthesize quantum nanowires networks [4, 5]. From the fundamental point of view, quantum graphs have become a test bed for studying different aspects in quantum mechanics and, due to the complex nature of the problem, the development of a unique method that holds for all graphs is difficult. Fortunately, however, there are some techniques developed in the literature that are able to deal with this problem [6]. Among the several methods to deal with quantum graphs, an interesting one is the Green's function approach, first proposed in [7] and further explored in [8, 9]. In this work we shall deal with specific scattering properties of quantum graphs, which are identified by two leads and sets of vertices and edges, to be described in the next section. The focus is mainly on the transmission properties of simple graphs, owing to the possibility of applications of physical interest. We investigate the global transmission amplitude of quantum graphs as a function of the wave number of the incident signal using the Green's function approach developed in [8, 9]. In particular, closer attention is given to the Braess paradox [10], and the possibility to identify regions of wave numbers in which the transmission coefficient increases significantly, searching for the presence of peaks of constructive quantum interference of very narrow width, similar to Feshbach resonances [11], in distinct arrangements of the two basic structures to be studied in this work.

As one knows, the Braess paradox was first discussed by Dietrich Braess in 1968 [10], and further studied in Refs. [12, 13]. Originally, it showed that adding an extra road to

a congested road traffic network to improve traffic flow may sometimes have the reverse effect, impeding the flow. In this work we follow the interpretation that the addition of a new possibility may under specific conditions enlarge the complexity of the system, opening new possibilities that may include surprisingly unexpected responses. The paradox may appear at the classical or quantum level, and it was also discussed in several other contexts in Refs. [14–19], in particular in [14], in which numerical simulations of quantum transport in mesoscopic networks with two and three branches reveals the transport inefficiency, which is further confirmed by a scanning-probe experiment using a biased tip that modulates the conductance variation in terms of the tip voltage and position. Moreover, it also appears in [15] in a numerical simulation in a quantum ring of finite width with the addition of a central horizontal branch, in [18] in the context of electronic transport in two quantum dots that are coupled together with two and three leads, and in [19] in the case of a phase-coherent quantum transport through a simple three-arm metallic fork. As we shall show, the Braess paradox also appears related to the global transmission of the quantum graphs that we examine in the current work.

Besides exploring global transmission properties of quantum graphs, we also concentrate on the presence of very narrow peaks of full transmission. The narrowness of the peaks reminds us of Feshbach resonances [11], which, in the context of quantum graphs, were investigated before in Ref. [20] in a ring graph with edges with unequal sizes. The effect that we are interested here is different, that is, we search for peaks of full transmission that we call peaks of constructive quantum interference, which occur inside regions of no transmission. The search for the Braess paradox in simple quantum graphs is an important motivation of the current work, but since it is related to the presence of complexity, we also concentrate on the construction of composed devices to provide the existence of very narrow peaks of constructive quantum interference.

We deal with quantum graphs, but in this work we consider simple graphs that are formed by arrangements of ideal leads, edges and vertices. This means that neither the vertices nor the leads and edges allow for dissipation of information and, in this sense, any linear arrangement of leads, edges and vertices is trivial, since it gives full global transmission (see

---

\* alexandrinko@gmail.com

† fmandrade@uepg.br

‡ bazeia@fisica.ufpb.br

below). To go further on out of the trivial situation, we have to consider the possibility of a vertex being connected by a triple junction, in the form of a Y-shaped configuration, which is usually called a vertex of degree 3. In this case, the signal reaching a vertex has the possibility to reflect and return, and two possible paths of transmission, and this introduces non-trivial quantum effects that can appear in the global transmission coefficient of the graph. Of course, there is a diversity of possibilities of constructing graphs with vertices connected by two, three, four and more edges, and so in this work we consider the two simple possibilities of hexagonal arrangements composed of two leads, six vertices and eight edges, with all the vertices having degree 3. We consider this possibility in order to eliminate effects that could appear due to the presence of vertices with higher degrees, which seem to prefer back-scattering [21]. We call this the degree 3 condition, and use it to simplify the current investigation.

The presence of vertices of degree 3 leads us with two distinct graphs that can be used to build arrangements that gives interesting responses, which can be of practical use in the construction of simple devices with important quantum properties. The two graphs to be considered in this work are hexagonal graphs with some internal structure, and this will also be of current interest, since hexagons are important to tile the plane to lead to hexagonal structures with vertices of degree 3, which are important part in nanotubes [22], in graphene sheets [23, 24] and in carbon boron nitride hybrid nanosheets [25]. In this sense, the current investigation may also attract interest toward graphene, nanotubes and other related structures. Nanotubes, in particular, are two-dimensional hexagonal lattices of carbon atoms arranged to form hollow cylinders. They may be arranged in three distinct ways, having the armchair, zig-zag or chiral conformation, and may be metallic or semiconductor, so the spatial conformation induces distinct electronic transport properties.

In order to deal with the above issues and implement the investigation, we organize the work as follows. In the next Sec. II, the main properties of quantum graphs are described, and there one concentrates mainly on the global transmission of simple graphs via the Green's function approach. In the Sec. III we introduce the two main graphs to be studied in this work, and there we describe and compare their global transmission coefficients. This investigation allows that we identify the Braess paradox. Since the paradox indicates the presence of quantum complexity, in Sec. IV we deal with some simple composition of these two graphs and study some simple series and parallel arrangements of them. This will lead us to the presence of narrow peaks of full transmission, so in Sec. V we further investigate the issue to search for the presence of very narrow peaks of constructive quantum interference. In Sec. VI we end the work, adding some comments and conclusions, paying further attention to the possibility of using the results of the work to applications of current interest to the area of quantum information. In particular, in the companion Letter [26] we examine simpler possibilities to propose the fabrication of devices to support the control of information at the quantum level.

## II. PROCEDURE

In this section, we review some concepts of graphs as used in this paper. In particular, we deal with quantum effects and the use of the Green's function approach for the calculation of the global transmission properties of quantum graphs, paying closer attention to the case of graphs with simple arrangements of leads, edges and vertices.

### A. Quantum graphs

A graph  $G(V, E)$  consists of a set of vertices  $V(G) = \{1, \dots, n\}$  and a set of edges  $E(G) = \{e_1, \dots, e_l\}$  [27]. The graph is described in terms of the adjacency matrix  $A(G)$  of dimension  $n \times n$  where the  $ij$ th element is defined by

$$A_{ij}(G) = \begin{cases} 1, & \text{if } \{i, j\} \in E(G), \\ 0, & \text{otherwise.} \end{cases} \quad (1)$$

The degree of a vertex  $i$  is defined as  $d_i = \sum_{j=1}^n A_{ij}(G)$ . We denote the set of neighbors of a vertex  $i$  by  $E_i = \{j : e_s = \{i, j\} \in E(G)\}$  and the set of neighbors of  $i$  but with the vertices  $\{k_1, \dots, k_{d_i}\}$  excluded by  $E_i^{k_1, \dots, k_{d_i}} = E_i \setminus \{k_1, \dots, k_{d_i}\}$ . A metric graph  $\Gamma(V, E)$  is a graph in which is assigned a positive length  $\ell_{e_s} \in (0, +\infty)$  to each edge. When a single ended edge  $e_s$  is taken as semi-infinite ( $\ell_{e_s} = +\infty$ ), it is called a *lead*. A quantum graph is a metric graph in which is possible to define a Schrödinger operator along with appropriated boundary conditions at the vertices [2]. In general, the Schrödinger operator along the edge  $\{i, j\}$  has the form

$$H_{ij} = -\frac{\hbar^2}{2m} \frac{d^2}{dx^2} + V_{ij}(x), \quad (2)$$

where  $V_{ij}(x)$  is the corresponding potential. In this sense, we can model distinct edges with the inclusion of different potentials; in particular, one can add a square well which will modify the transmission through the edge and so the global transmission through the graph. In this work, however, we shall take  $V_{ij}(x) = 0$ , that is, we shall use the free Schrödinger operator.

### B. The Green's function approach

In the context of quantum graphs, the exact scattering Green's function for a quantum particle of fixed energy  $E = \hbar^2 k^2 / 2m$ , with initial position  $x_i$  in the lead  $e_i$  and final position  $x_n$  in the lead  $e_n$  is given by a sum over all the scattering paths connecting the points  $x_i$  and  $x_n$ , where each path is weighted by the product of the scattering amplitudes gained along the path [8]. The reflection and transmission amplitudes,  $r_i$  and  $t_i$ , at the vertex  $i$ , are determined through the boundary conditions defined at the vertex  $i$ . With the help of the adjacency matrix of the graph, it was shown in [9] that this

sum over the paths can be written in the form

$$G_{\Gamma_{in}} = \frac{m}{i\hbar^2 k} T_{\Gamma_{in}}(k) e^{ik(x_i + x_n)}, \quad (3)$$

where

$$T_{\Gamma_{in}}(k) = \sum_{j \in E_i} t_i A_{ij} p_{ij}^{(n)}, \quad (4)$$

is the *transmission amplitude*. The  $p_{ij}^{(n)}$  is the family of paths between the vertices  $i$  and  $j$ , which are given by

$$p_{ij}^{(n)} = z_{ij} r_j p_{ji}^{(n)} + \sum_{l \in E_j^{i,n}} z_{ij} t_j A_{jl} p_{jl}^{(n)} + z_{ij} t_n \delta_{jn}, \quad (5)$$

with  $z_{ij} = e^{ik\ell_{\{i,j\}}}$ . The family  $p_{ji}^{(n)}$  is given by the same expression above, but with the swapping of indices  $i$  and  $j$ . Then, in each vertex  $i$  we associated one  $p_{ij}^{(n)}$  for every  $j \in E_i$ . In this work, we shall employ the above approach to determine the *transmission coefficient*  $|T_{\Gamma_{in}}(k)|^2$  for different quantum graphs and then discuss their properties. We shall consider equilateral quantum graphs where the length of all the edges are the same and set them to  $\ell$ , such that  $z_{ij} = z = e^{ik\ell}$ .

### C. The quantum amplitudes

Let us now discuss about the possible boundary conditions. As one knows, a commonly vertex condition used is the so-called  $\delta$ -type condition defined by [28]

$$\begin{aligned} \psi_{\{i,j\}} &= \varphi_j, & \forall i \in E_j, \\ \sum_{i \in E_j} \psi'_{\{i,j\}} &= \alpha_j \varphi_j, \end{aligned} \quad (6)$$

where  $\varphi_j$  is the value of the wave function at the vertex  $j$  and  $\alpha_j$  is real parameter related to the strength of the  $\delta$ -type interaction. The prime in (6) represents the derivative, which should be taken in the outgoing direction, i.e., from the vertex into the edges or leads. Using this boundary condition the quantum amplitudes have the form [8, 9]

$$r_j(k) = \frac{\alpha_j - (d_j - 2)ik}{ikd_j - \alpha_j}, \quad (7)$$

$$t_j(k) = \frac{2ik}{ikd_j - \alpha_j}. \quad (8)$$

Among the choices for the value of  $\alpha_i$ , an interesting one is  $\alpha_i = 0, \forall i$ . In this case, we are considering no barrier at the vertices, resulting in the so-called Neumann-Kirchhoff boundary condition. As a result, the quantum amplitudes have the property of being independent of  $k$ ,

$$r_j = \frac{2}{d_j} - 1, \quad t_j = \frac{2}{d_j}, \quad (9)$$

showing that the reflection amplitude increases with the increasing of the degree of the vertex. When a Neumann-Kirchhoff boundary condition is used at a vertex of degree



FIG. 1. (Color online) Illustration of the diamond and hexagonal graphs.

2, the transmission amplitude is equal to 1 and the vertex becomes an ordinary point joining the edges. Such vertices are called Neumann vertices [2]. In what follows, we shall adopt Neumann vertices of degree 3. In this case the reflection and transmission amplitudes are explicitly given by  $r_i = -1/3$  and  $t_i = 2/3$ , respectively.

With the above conditions, we shall be then considering quantum graphs with ideal leads and edges, and with vertices that obey the Neumann boundary conditions. This is the simplest possibility, and we shall also only consider vertices of degree 3, to avoid accounting for effects due to vertices of different degrees.

### III. SIMPLE GRAPHS

Let us now concentrate on simple graphs. One uses the symbol  $\bullet$  to represent vertices, and straight line segments to stand for the edges and leads, and first considers the graph  $\bullet\text{---}\bullet$  with two leads, one at the left and the other at the right of the vertex. As we have already commented, this is trivial and gives  $|T_{\bullet\text{---}\bullet}(k)|^2 = 1$ , since we are considering a Neumann vertex. If we go further and consider the graph  $\bullet\text{---}\bullet\text{---}\bullet$  we also get full transmission,  $|T_{\bullet\text{---}\bullet\text{---}\bullet}(k)|^2 = 1$ . In view of this, we have to consider vertices with higher degrees leading to more complex graphs to open the possibility of having nontrivial transmission effects, so we depict the diamond ( $D$ ) and the hexagonal ( $H$ ) graphs that are shown in Fig. 1. In this case, the transmission amplitudes can be written as

$$T_D(k) = \frac{8z^2}{9 - z^4}, \quad (10)$$

$$T_H(k) = \frac{8z^3}{9 - z^6}, \quad (11)$$

and the corresponding transmissions coefficients are shown in Fig. 2.

The transmission coefficients are nontrivial anymore, and the effects are due to the presence of the left and right vertices of degree 3. Here we notice that since we are considering Neumann vertices, the difference between the diamond and hexagonal graphs depicted in Fig. 1 is only due to the difference between the two internal paths, which is at the ratio  $2/3$ , as it nicely appears when one accounts for the difference between the periodicity of the transmission of the diamond and the hexagonal graphs that appear in Fig. 2.

Since the presence of vertices of degree 3 induces nontrivial transmission, we then focus on this and consider the new graphs which are depicted in Fig. 3. They are all constructed with vertices of degree 3 in the diamond and hexagonal families. Since there is only one graph in the diamond family,

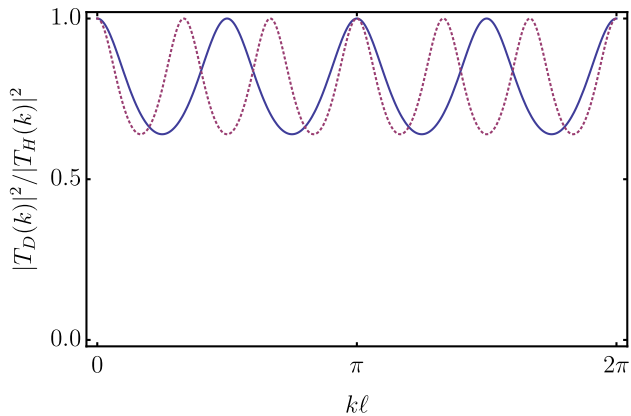


FIG. 2. (Color online) Transmission coefficients of the diamond (blue solid line) and hexagonal (violet dotted line) graphs shown in Fig. 1.

we cannot compare the transmission behavior of two distinct diamond graphs with vertices of degree 3. Due to this, from now on we concentrate on the transmission coefficient of the two graphs of the hexagonal family, to compare their properties. This means that our results will not be contaminated by effects of vertices of different degrees.

We represent the two different square and crossed hexagonal graphs by  $Q$  and  $X$ , respectively. The transmission amplitudes for these two graphs are given by

$$T_Q(k) = \frac{32z^3(1+z)}{(9+4z^2+3z^4)(9-3z+z^2-3z^3)}, \quad (12)$$

$$T_X(k) = \frac{64z^3}{81+9z^2-17z^4-9z^6}, \quad (13)$$

and the corresponding transmission coefficients are displayed in Fig. 4, unveiling interesting nontrivial properties which we discuss below.

As we noted, the two transmission coefficients are periodic so we display them in Fig. 4 for the wave number in the interval of periodicity of the  $Q$  graph. We also observe that the transmission coefficient of the  $Q$  graph is more complex than the other one. More importantly, it may vanish in a large interval which we call the suppression band, inside its interval of periodicity. The results also show that there are regions in  $k$  space, where the transmission is more or less significant for the  $Q$  than the  $X$  graphs. That is,  $|T_Q(k)|^2$  may be greater

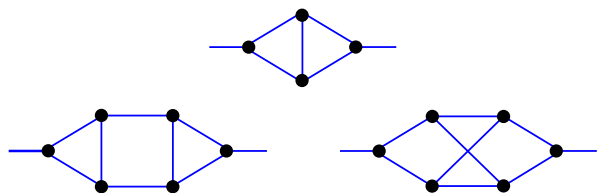


FIG. 3. (Color online) Graphs with vertices of degree 3 in the diamond and hexagonal families.

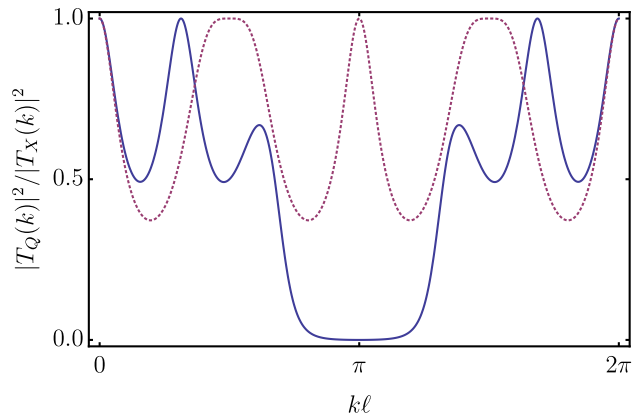


FIG. 4. (Color online) Transmission coefficients of the two structures, the hexagonal square (blue solid line) and crossed (violet dotted line) arrangements  $Q$  and  $X$  that appear in Fig. 3.

(smaller) than  $|T_X(k)|^2$ , depending of the interval in  $k$  space in consideration.

This opens the interesting possibility to study the presence of the Braess paradox in those quantum graphs. The paradox was first discussed by Braess in 1968 [10]; see also [12, 13]. It was also studied in several other contexts in Refs. [14–18], and in [19] in the context of quantum graphs. Here we depict the difference  $|T_Q(k)|^2 - |T_X(k)|^2$  between the two coefficients, to see regions where one is higher than the other. This is shown in Fig. 5, and we can observe that for  $k\ell$  in the interval  $1.15215 < k\ell < 5.13103$  the transmission of the  $X$  graph is higher than the transmission of the  $Q$  graph. However, for  $0 < k\ell < 1.15215$  and for  $5.13103 < k\ell < 2\pi$  one sees that the transmission for the  $Q$  graph is greater than the one for the  $X$  graph, and this is a manifestation of the Braess paradox.

To see that this is indeed the case, let us first discuss the problem classically: one supposes that a classical signal (a soccer ball, for instance) enters the graph at the left (right) lead and leaves it at the right (left) lead; one notices from Fig. 3 that for the  $Q$  graph the shortest trajectory requires three steps, and that there are two distinct possibilities; for the  $X$  graph, the shortest trajectory also requires three steps, but now there are four distinct possibilities. Thus, the transmission through the  $X$  graph seems to be more efficient than the other one. However, the problem is more complex than this, because of the presence of reflection at the vertices. For instance, the next shortest trajectory for the  $Q$  graph requires four steps, and there are four possibilities; for the  $X$  graph there is no trajectory with four steps. In fact, the  $X$  graph has only trajectories with odd number of steps, whereas the  $Q$  graph has both even and odd number of steps. This difference between these two graphs is reflected in the values of the respective classical hitting times (see below), which are calculated numerically to give  $h_Q^c = 13.57143$  and  $h_X^c = 12.84615$ . These results inform us that classically one should expect higher flux through the  $X$  graph.

Since we are interested in quantum graphs, let us then direct

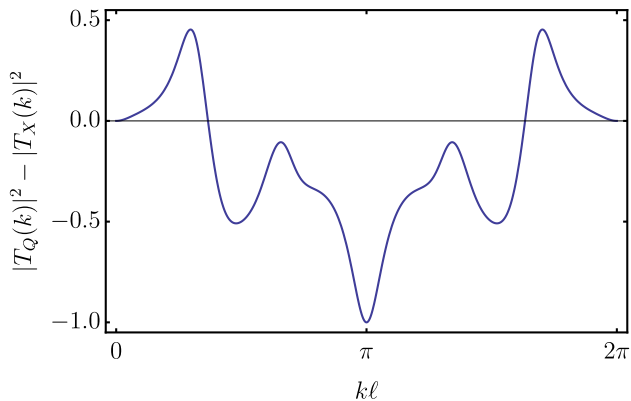


FIG. 5. (Color online) The difference between the transmission coefficients of the  $Q$  and  $X$  graphs.

the investigation to the quantum level. To do this, we take advantage of the quantum hitting time (see below) related to the two graphs  $Q$  and  $X$ . The numerical calculation of the quantum hitting time gives  $h_Q = 4.01196$  and  $h_X = 13/4 = 3.25$ . These results show that the quantum transmission through the  $X$  graph is expected to be more efficient than the one through the  $Q$  graph in general. However, due to the quantum complexity of the two graphs, there are regions of wave numbers where the transmission through the  $Q$  graph is more efficient than the one of the  $X$  graph, and this is a clear manifestation of the Braess paradox.

The numerical calculation of the hitting time is based on the fact that, in the context of random walks on graphs, the concept of hitting time is directly related to the expected number of steps to reach the vertex  $f$  starting from a vertex  $i$  [29]. This concept can be extended to the realm of quantum mechanics in the context of quantum walks, which are the quantum version of random walks [30]. So, the corresponding quantity for a quantum walk is the expected number of steps to reach the quantum state in the edge  $e_n$  starting in the state in the edge  $e_i$  [31, 32]. Actually, quantum walks and quantum graphs are deeply related to each other [33] and this relation was further explored in [34]. Based on results of [34], it turns out that the Green's function for a quantum graph is actually a *generating function* for all the possible walks leaving the entrance lead and getting the exit lead in the scattering process. In this manner, the term  $z = e^{ik\ell}$  is equivalent to a time step in the quantum walk problem. So, to extract all the paths with exactly  $m$  steps we use the *step operator* [34]

$$\hat{S}_m = \frac{1}{m!} \left. \frac{\partial^m}{\partial z^m} \right|_{z=0}. \quad (14)$$

Thus, the total probability for the quantum walker to leave the entrance lead and to get the exit lead of the graph in exactly  $m$  steps in the scattering process is

$$P(m) = |\hat{S}_m T_{\Gamma_{in}}|^2, \quad (15)$$

with  $T_{\Gamma_{in}}$  given by Eq. (4). Additionally, the probability to

measure the particle for the first time in the exit lead, regardless the number of steps,  $P_{out}$ , is given by

$$P_{out} = \sum_{m=1}^{\infty} P(m). \quad (16)$$

Then, it is possible to define a *conditional hitting time*,  $h$ , as [31, 32]

$$h = \frac{1}{P_{out}} \sum_{m=1}^{\infty} m P(m). \quad (17)$$

This is the definition employed for the calculation of  $h_Q$  of the  $Q$  graph and  $h_X$  of the  $X$  graph, as described above. The classical case is simpler, and we follow the same reasoning above for the computation of the classical hitting time, but using classical walks with transition probabilities of  $1/3$  at each vertex.

The presence of the Braess paradox in the current context informs us that both the  $Q$  and  $X$  graphs are complex enough to give rise to other effects of current interest for quantum information. They then motivate us to go further and explore other possibilities. In the current investigation we explore the fact that the  $Q$  graph engenders a band of no transmission in  $k$  space, as it is easily identified from the blue solid line depicted in Fig. 4. This is the suppression band, and it is an interesting and unexpected quantum effect that can be used in application of current interest. The simplest possibility is to use it to block the passage of information through the quantum graph, which can be seen as a device of direct interest to the construction of tools that allow for the control and manipulation of quantum information. Yet more interesting is to see the two quantum graphs as two independent quantum devices, which can be used to the construction of others, composed devices, and this will be investigated in the next Section.

## IV. GRAPH CIRCUITRY

Let us now use of the two quantum devices, the  $Q$  and the  $X$  graphs, to build compound structures and study their transmission properties at the light of the above investigation.

### A. Simple series circuits

We first consider the series composition, of the forms  $S(QQ)$ ,  $S(QX)$ ,  $S(XQ)$  and  $S(XX)$ , where  $S(QX)$  indicates the series composition of the graph  $Q$  with the graph  $X$ , keeping the degree 3 condition of the vertices, which in the series arrangement occurs very naturally. We then calculate and display the transmission coefficient for all the cases in Fig. 6. Although the square and crossed graphs are different, the compound transmission does not depend on the order one chooses each other, so we say that  $S(QX) = S(XQ)$ . We compare the transmission displayed with the blue solid line in Fig. 4 with the one in the top panel in Fig. 6 to see that the series composition of two square graphs enlarges a

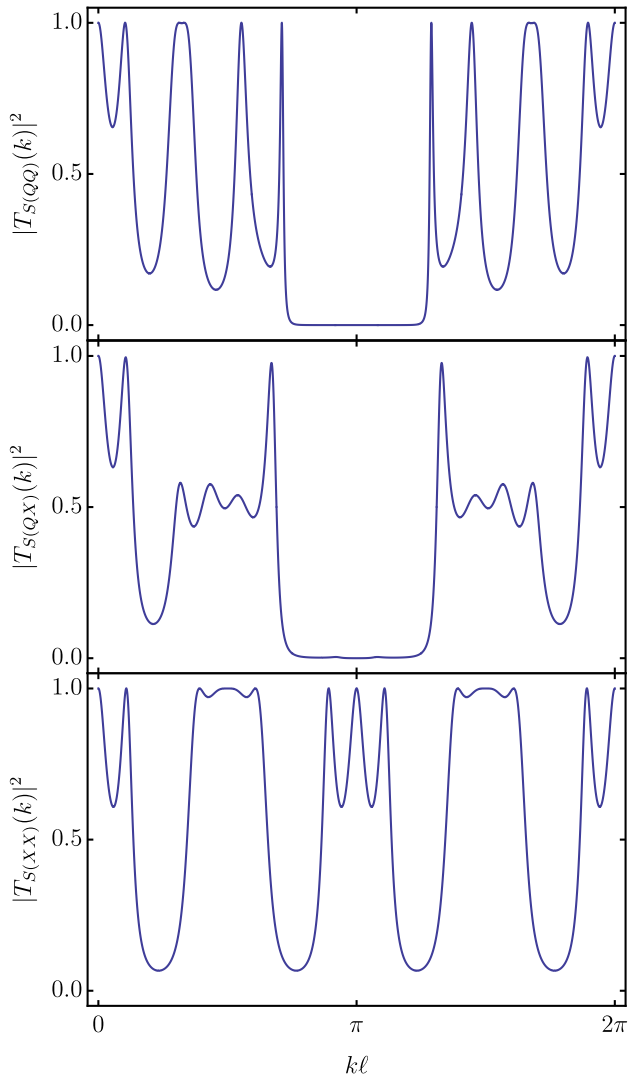


FIG. 6. (Color online) Transmission coefficients of the three compound structures, the series arrangements  $S(QQ)$ ,  $S(QX)$ , and  $S(XX)$ , depicted from top to bottom, respectively.

bit the suppression band in  $k$  space around  $k\ell = \pi$ , so it is a bit more efficient to block the passage of information. On the other hand, the violet dotted line that appear in Fig. 4 and the bottom panel in Fig. 6 show the appearance of extra maxima in the transmission coefficient of the  $S(XX)$  graph. This composition also deepens the main minima, approaching them to suppression. The composition  $S(QX)$  which appears in the middle panel in Fig. 6 is also interesting: it shows an almost invisible substructure in the suppression band, and this suggests that we further explore this effect.

To do this, we add another basic device to the series structure, so we consider compound structures with three devices. In this case there are several possibilities and in Fig. 7 we depict the three series arrangements  $S(QQQ)$ ,  $S(QXQ)$  and  $S(XXX)$ , which are important for the considerations that follow below. The top and bottom panels in Fig. 7 show a be-

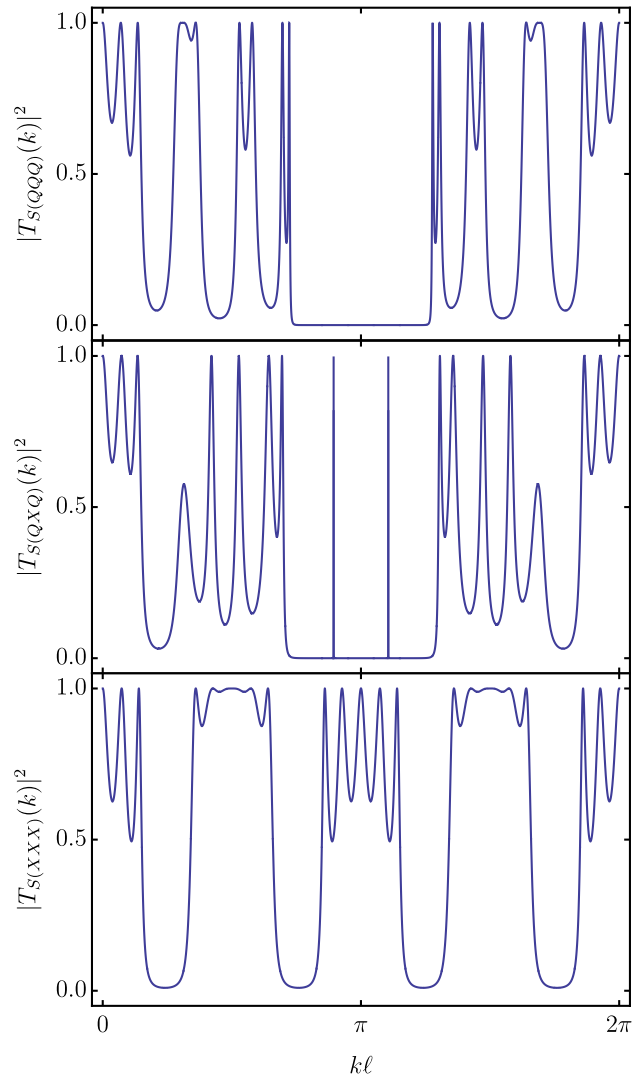


FIG. 7. (Color online) Transmission coefficients of the three compound structures, the series arrangements  $S(QQQ)$ ,  $S(QXQ)$ , and  $S(XXX)$ , depicted from top to bottom, respectively.

havior which appeared before, when we compared with Figs. 4 and 6. In particular, in the top panel in Fig. 7, one sees that the transmission coefficient vanishes completely in some interval in  $k$  space, so we can also use this in applications of current interest. Moreover, the behavior that appears in the middle panel in Fig. 7 reveals an unexpected quantum behavior, the presence of two very narrow peaks of full transmission inside the suppression band. They are very interesting and are consequences of the constructive quantum interference in the underlying graph, which we further study in Sec. V.

## B. Simple parallel circuits

Let us now study the case of parallel circuits. Here the condition that we only have vertices of degree 3 selects some spe-

cific combinations of the elementary devices. The simplest parallel possibilities are the  $P(QQ)$ ,  $P(QX) = P(XQ)$  and  $P(XX)$  structures, where  $P$  is used to indicate parallel arrangements. The  $P(QX)$  arrangement, for instance, is constructed as follows: one puts the  $Q$  graph on top of the  $X$  graph, without contact, and at the center of the vertical arrangement, at the left and right one adds two extra vertices, the one at the left (right) being connected with a left (right) lead, and then connected with two other edges to keep the degree 3 condition, one going up to the  $Q$  graph, and the other going down to the  $X$  graph.

We study the three distinct possibilities and in Fig. 8 we depict the transmission coefficients for the three distinct cases. We note that both the top  $P(QQ)$  and bottom  $P(XX)$  figures give results somehow similar to the respective cases in the series arrangements shown in Fig. 6; compare the top results and the bottom results of both Figs. 6 and 8. However, the middle panel which describes the  $P(QX)$  possibility is different from the case displayed in the middle panel of Fig. 6, so we go further and study other compositions.

### C. Other arrangements

The above results suggest that we study other possibilities. The series and parallel arrangements are more intricate than the elementary  $Q$  and  $X$  compositions, and they require more complicate numerical calculations. However, if one keeps the condition of vertices of degree 3, there are several possibilities and we can, for instance, consider the parallel structures  $P(QQ)$ ,  $P(QX)$  and  $P(XX)$  in parallel and in series. Examples are the cases  $P(P(QQ)P(QX))$  and  $P(P(QX)P(XQ))$ , which represent parallel arrangements of parallel arrangements, etc, and  $S(P(QQ)P(XX)P(QQ))$ , which represents a series arrangement of three parallel arrangements, etc.

We have studied several cases and in comparison with the previous results, we found no qualitatively different behavior. To exemplify the findings, let us consider for instance the case of a parallel composition of two parallel compositions and a series composition with three structures of two parallel compositions. The results are depicted in Fig. 9, for the cases  $P(P(QX)P(XQ))$  and  $S(P(QQ)P(XX)P(QQ))$ , respectively. We note that the transmission coefficients for these new compositions add no different qualitative effects, in comparison with the previous results, so we end the calculations of transmission coefficients here.

## V. INTERFERENCE

We see from the transmission coefficients of the several arrangements already studied, the appearance of peaks of full transmission in the region around the center ( $k\ell = \pi$ ) of the periodic region in  $k$  space, which we now want to investigate more carefully. We first focus on the central peak that is displayed with the violet dotted line in Fig. 4. We do this by looking at the poles of the Green's function which,

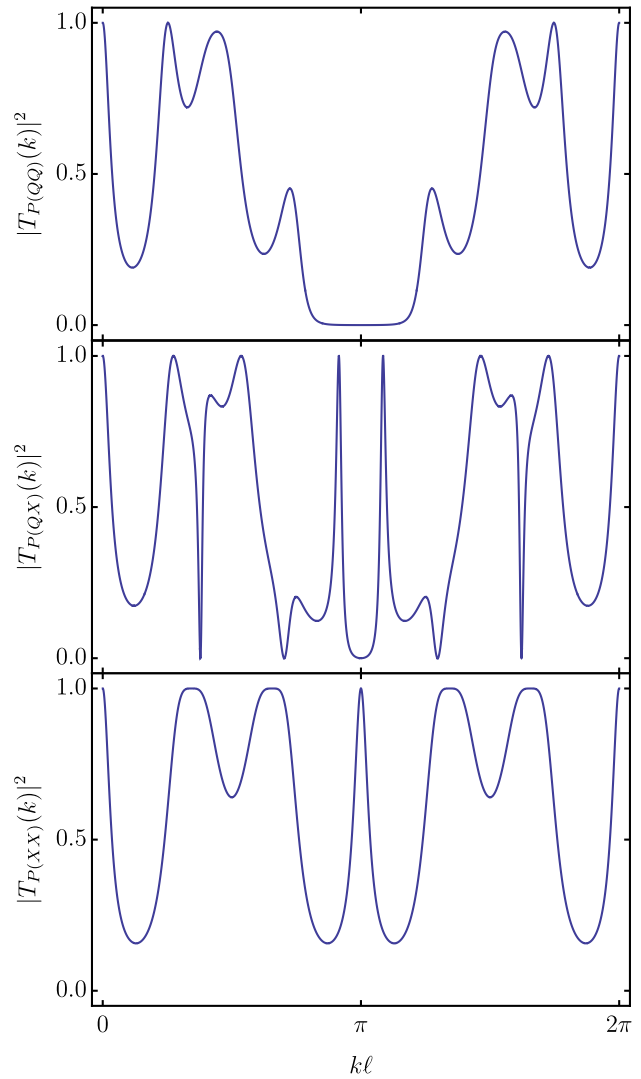


FIG. 8. (Color online) Transmission coefficients of the three compound structures, the parallel arrangements  $P(QQ)$ ,  $P(QX)$ , and  $P(XX)$ , depicted from top to bottom, respectively.

for the  $X$  graph depicted in Fig. 3 are all contained in the roots of the denominator of Eq. (13) [8]. Here we identified a pole at  $k\ell = \pi$ , so one extends the investigation to the complex plane to find that this pole has a width that measures  $w_X = 0.54408$ . Similarly, we also confirmed the presence of the pole at  $k\ell = \pi$  in the bottom panel in Fig. 6, but now the width is  $w_{S(XX)} = 0.25037$ .

The more interesting and unexpected case appears from the middle panel in Fig. 7 and in the bottom panel in Fig. 9. There are two similar peaks which engender very narrow widths, so we further examine the corresponding Green's function and find the two poles that appear in the middle panel in Fig. 7: they are located at  $k\ell = \pi \pm 0.3325$ , and have very narrow width, which obeys  $w < 0.0003$ . They are peaks of full transmission that appear inside the band of full suppression, and can be interpreted as peaks of constructive quantum interfer-

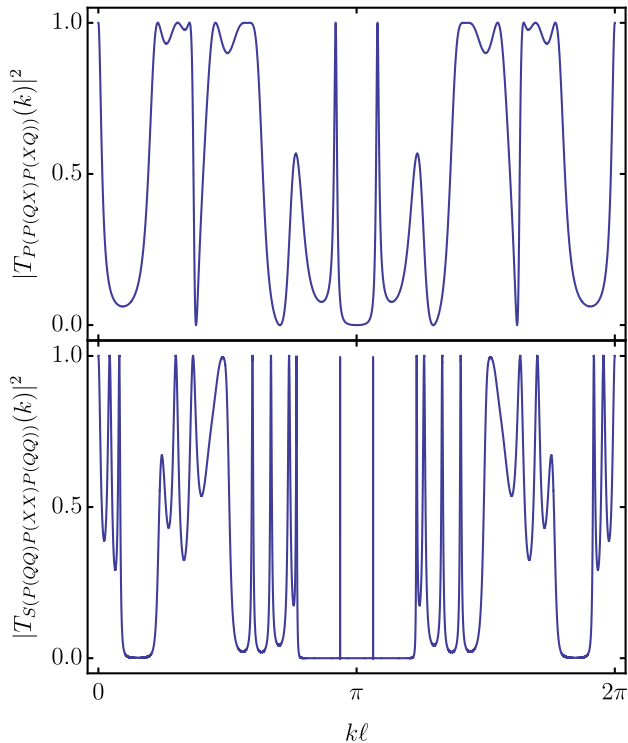


FIG. 9. (Color online) Transmission coefficients of two compound structures, the parallel arrangement of two parallel structures,  $P(P(QX)P(XQ))$ , and the series arrangements of three parallel structures  $S(P(QQ)P(XX)P(QQ))$ , depicted from top to bottom, respectively.

ence. A similar situation appears in the bottom panel in Fig. 9. The presence of the two peaks symmetrically located around  $k\ell = \pi$  is a consequence of the time reversal symmetry of the quantum graphs, which do not distinguish the signal entering from the left (right) and leaving to the right (left). Note that the time reversal symmetry is present in all graphs here studied; It shows that  $|T(\pi + k\ell)|^2 = |T(\pi - k\ell)|^2$ , for  $k\ell \in [0, \pi]$ , for all the global transmission coefficients.

## VI. DISCUSSION

In this work we studied global transmission properties of two simple quantum graphs in the family of hexagonal graphs. The two graphs appeared in the study of simple graphs that engender nontrivial behavior, and they are all constructed under the condition that the vertices are of degree 3. This condition is imposed to circumvent the presence of effects due to vertices of different degrees, that could perhaps complicate the understanding of the results.

With this condition at hand, we ended up with the two quantum graphs of the hexagonal family which are displayed in Fig. 3, represented by  $Q$  and  $X$ , respectively. We calculated the corresponding global transmission coefficients  $|T_Q(k)|^2$  and  $|T_X(k)|^2$  and examined some of their properties. In

particular, we showed the presence of the Braess paradox, since the difference between the two global transmissions  $|T_Q(k)|^2 - |T_X(k)|^2$  displayed in Fig. 5 can be positive or negative, depending on the value of the incoming wave number. To probe on this issue, we relied on the calculation of the hitting time for the two graphs, at the classical and quantum levels, and in both cases the results showed that the hitting time for the  $Q$  graph is greater than the one for the  $X$  graph.

We also found a surprising and unexpected quantum behavior, which concerns the presence of a suppression band, that is, a large region in wave number, where the global transmission of information is fully suppressed by the  $Q$  graph. Motivated by this and the results on the Braess paradox, which is in this work interpreted as being due to the complex character of the two quantum graphs, we explored other possibilities, using the two graphs as elementary devices that could be added together in series and/or parallel, to form composed structures. We studied several arrangements, finding results that can certainly motivate the construction of apparatus of current interest for the transmission of quantum information. Also surprising, we showed how to compose the elementary devices to find very narrow peaks of constructive quantum interference inside the suppression band of the  $Q$  device. We investigated the values and widths of these peaks and showed that they are indeed very narrow.

If one thinks of the two quantum graphs as two elementary devices, it is possible to probe them following the lines of Ref. [3], in which experimental and theoretical results show that microwave networks can simulate quantum graphs with time reversal symmetry. This is an interesting line of investigation, and is further connected with another very recent investigation [35] on graphs and possible simulations via microwave networks. One can also think of considering networks of fibers and splitters, as considered in [36]. In this case, in the simplified version we may say that when a signal reaches a splitter, it is transmitted towards one of the connected fibers chosen at random, with the transition probability given in terms of splitting factors, with the information flowing as a random walk on the graph [36, 37].

Another important line of research concerns the construction of quantum devices at the nanometric scale, simulating the two quantum graphs  $Q$  and  $X$  with quantum dots connected by edges and leads; see, e.g., [4, 5] and references therein. The idea is to suppose that electrons in the incoming lead reach a quantum dot from one side and leave the device through the quantum dot at the outgoing lead on the other side, after interacting with the four other quantum dots that are arranged to form the two hexagonal graphs displayed in Fig. 3. Here the matter flow can be controlled by chemical potentials of electronic sources that are attached to the left and right leads. Although this seems to be a challenge at the experimental level, a simpler composition was suggested before in [18], in an arrangement with two quantum dots that also unveiled the Braess paradox. The quantum dot composition suggested in [18] and the Braess paradox that appeared in the transmission results there obtained strongly motivate new research in the subject.

From the practical perspective, the experimental construc-



tion of devices based on quantum dots seems to face another challenging obstacle, which concerns the graph  $X$ , that requires two edges that cross without touching each other. To circumvent this, one has to leave the planar perspective to build spatial devices. There is no problem here, if one thinks of modelling microwave structures like the ones described in [3, 35] and also, the fabrication of lattices of optical fibers and splitters in the form recently suggested in [36, 37]. Moreover, we can think of using the procedure described in the current work to model nanotubes [22] and graphene sheets [23]. Nanotubes, for instance, may be of the arm-chair, zig-zag or chiral type, with the cylindrical conformation inducing distinct electric properties, so it would be of current interest to investigate the corresponding transmission coefficients under the lines of the present work. Another possibility of practical interest is to leave the  $Q$  and  $X$  arrangements and examine simpler graphs, with the focus on the construction of simpler quantum devices at the nanometric scale. The challenge here is to conciliate quantum complexity with geometric simplicity, complexity that is required for the description of the Braess paradox and the presence of quantum interference, and simplicity which is welcome for the fabrication of quantum devices. A proposal of current interest is explored in the companion Letter [26], where we deal with simpler graphs, which, despite the geometric simplicity, still produce quantum complexity enough to reveal the Braess paradox and the presence of constructive quantum interference.

The theoretical perspective engenders other realisations, an interesting one being the study of more realistic graphs. A feasible possibility is the inclusion of potentials along the edges and/or barriers at the vertices of the quantum graphs. This can

be implemented with the addition of real parameters related to the potentials added along the edges, as commented on below Eq. (2), and the strength of the  $\delta$ -type interaction at the vertices; this last possibility is controlled by Eqs. (6), (7) and (8), and its realization follows straightforwardly. In the case of electronic transport of information, we can also add appropriate magnetic fields, which would break the time reversal symmetry and add new effects. Another line of investigation concerns the search for other graphs, with similar properties but distinct topologies, which could suggest the construction of other experimental devices of direct interest to the control and manipulation of quantum information. We are now elaborating on some of the above issues, hoping to report on them in the near future.

## ACKNOWLEDGMENTS

This work was partially supported by the Brazilian agencies Conselho Nacional de Desenvolvimento Científico e Tecnológico (CNPq), Fundação Araucária (FAPPR, Grant 09/2016), Instituto Nacional de Ciência e Tecnologia de Informação Quântica (INCT-IQ), and Paraíba State Research Foundation (FAPESQ-PB, Grant 0015/2019). It was also financed in part by the Coordenação de Aperfeiçoamento de Pessoal de Nível Superior (CAPES, Finance Code 001). FMA and DB also acknowledge CNPq Grants 313274/2017-7 (FMA), 434134/2018-0 (FMA), 306614/2014-6 (DB) and 404913/2018-0 (DB).

- 
- [1] T. Kottos and U. Smilansky, *Ann. Phys. (NY)* **274**, 76 (1999).  
 [2] S. Gnutzmann and U. Smilansky, *Adv. Phys.* **55**, 527 (2006).  
 [3] O. Hul, S. Bauch, P. Pakoński, N. Savytsky, K. Życzkowski, and L. Sirko, *Phys. Rev. E* **69**, 056205 (2004).  
 [4] K. A. Dick, K. Deppert, M. W. Larsson, T. Mårtensson, W. Seifert, L. R. Wallenberg, and L. Samuelson, *Nat. Mater.* **3**, 380 (2004).  
 [5] K. Heo, E. Cho, J.-E. Yang, M.-H. Kim, M. Lee, B. Y. Lee, S. G. Kwon, M.-S. Lee, M.-H. Jo, H.-J. Choi, T. Hyeon, and S. Hong, *Nano Lett.* **8**, 4523 (2008).  
 [6] G. Berkolaiko and P. Kuchment, *Introduction to Quantum Graphs* (American Mathematical Society, 2012).  
 [7] A. G. M. Schmidt, B. K. Cheng, and M. G. E. da Luz, *J. Phys. A* **36**, L545 (2003).  
 [8] F. M. Andrade, A. G. M. Schmidt, E. Vicentini, B. K. Cheng, and M. G. E. da Luz, *Phys. Rep.* **647**, 1 (2016).  
 [9] F. M. Andrade and S. Severini, *Phys. Rev. A* **98**, 062107 (2018).  
 [10] D. Braess, *Unternehmensforschung Operations Research* **12**, 258 (1968).  
 [11] H. Feshbach, *Ann. Phys. (NY)* **5**, 357 (1958).  
 [12] D. Braess, A. Nagurny, and T. Wakolbinger, *Transportation Science* **39**, 446 (2005).  
 [13] H. Youn, M. T. Gastner, and H. Jeong, *Phys. Rev. Lett.* **101**, 128701 (2008).  
 [14] M. G. Pala, S. Baltazar, P. Liu, H. Sellier, B. Hackens, F. Martins, V. Bayot, X. Wallart, L. Desplanque, and S. Huant, *Phys. Rev. Lett.* **108**, 076802 (2012).  
 [15] A. A. Sousa, A. Chaves, G. A. Farias, and F. M. Peeters, *Phys. Rev. B* **88**, 245417 (2013).  
 [16] J. E. Cohen and P. Horowitz, *Nature* **352**, 699 (1991).  
 [17] C. M. Penchina and L. J. Penchina, *Am. J. Phys.* **71**, 479 (2003).  
 [18] A. L. R. Barbosa, D. Bazeia, and J. G. G. S. Ramos, *Phys. Rev. E* **90**, 042915 (2014).  
 [19] E. Zhitlukhina, M. Belogolovskii, N. D. Leo, M. Fretto, A. Sosso, and P. Seidel, *Int. J. Quantum Inf.* **15**, 1740011 (2017).  
 [20] D. Waltner and U. Smilansky, *Acta. Phys. Pol. A* **124**, 1087 (2013).  
 [21] J. M. Harrison, U. Smilansky, and B. Winn, *J. Phys. A* **40**, 14181 (2007).  
 [22] R. Saito, G. Dresselhaus, and M. S. Dresselhaus, *Physical Properties of Carbon Nanotubes* (Imperial College Press, 1998).  
 [23] A. H. C. Neto, F. Guinea, N. M. R. Peres, K. S. Novoselov, and A. K. Geim, *Rev. Mod. Phys.* **81**, 109 (2009).  
 [24] S. Gilje, S. Han, M. Wang, K. L. Wang, and R. B. Kaner, *Nano Lett.* **7**, 3394 (2007).  
 [25] F. Shayeganfar and R. Shahsavari, *Carbon* **99**, 523 (2016).  
 [26] A. Drinko, F. M. Andrade, and D. Bazeia, arXiv:1906.07782 (2019), <http://arxiv.org/abs/1906.07782v2>.  
 [27] R. Diestel, *Graph Theory*, 4th ed., Graduate Texts in Mathematics Vol. 173 (Springer, 2010).

- [28] P. Exner, [Phys. Rev. Lett.](#) **74**, 3503 (1995).
- [29] J. Kempe, [Probab. Theory Relat. Fields](#) **133**, 215 (2005).
- [30] J. Kempe, [Contemp. Phys.](#) **44**, 307 (2003).
- [31] E. Feldman and M. Hillery, [Phys. Lett. A](#) **324**, 277 (2004).
- [32] E. Feldman and M. Hillery, in *Coding Theory and Quantum Computing*, Contemporary Mathematics, Vol. 381, edited by D. Evans, J. Holt, C. Jones, K. Klintworth, B. Parshall, O. Pfister, and H. Ward (2005) p. 71, [quant-ph/0403066](#).
- [33] G. K. Tanner, in *Non-Linear Dynamics and Fundamental Interactions*, Vol. 213 (Springer-Verlag, 2006) Chap. From quantum graphs to quantum random walks, pp. 69–87.
- [34] F. M. Andrade and M. G. E. da Luz, [Phys. Rev. A](#) **84**, 042343 (2011).
- [35] M. Ławniczak, J. Lipovský, and L. Sirko, [Phys. Rev. Lett.](#) **122**, 140503 (2019).
- [36] S. Lepri, C. Trono, and G. Giacomelli, [Phys. Rev. Lett.](#) **118**, 123901 (2017).
- [37] G. Giacomelli, S. Lepri, and C. Trono, [Phys. Rev. A](#) **99**, 023841 (2019).